MSC/EMAS NONLINEAR TRANSIENT ANALYSES OF MULTITURN COILS WITH ATTACHED CIRCUITS

John R. Brauer and Charles R. Figer, Jr.
The MacNeal–Schwendler Corporation
Electromagnetics Applications Department
4300 W. Brown Deer Road
Milwaukee, WI 53223 USA

ABSTRACT

MSC/EMAS can be used to model multiturn nonlinear coils with attached circuits. The circuits are modeled by 0D finite elements, which can be attached to 1D line elements that represent multiturn windings. The 1D elements can then be MPCd to the 3D or 2D finite element model containing nonlinear magnetic material. The complete finite element model is analyzed by nonlinear transient Solution 305. Example computations of time–varying currents and electromagnetic fields are shown for an inductor, a transformer, and an induction motor. The induction motor solution is shown to be aided by the new ADAPT nonlinear transient method that is available in Version 2.5.

INTRODUCTION

Electromagnetic devices often contain ferromagnetic cores operating in the nonlinear or saturated portion of their B−H curves. The cores may also have significant eddy current losses, and are usually wound with coils with multiple turns of wire. Because of the interaction between the magnetic cores and the circuits attached to the coils, the ferromagnetic components and attached circuits must be analyzed simultaneously if the electrical engineer is to predict the device performance.

This paper presents new MSC/EMAS techniques that enable dynamic analysis of nonlinear multiturn coils with attached electric circuits. Unlike previous finite element techniques that obtained impedances for use in circuits to obtain currents and voltages [1], the MSC/EMAS techniques discussed here enable direct coupled analysis of a nonlinear magnetic component and the attached electric circuit. After discussing the new techniques, they are first applied to the nonlinear RLC circuit previously analyzed by circuit techniques. Other example analyses are a transformer and an induction motor.

ATTACHING CIRCUITS TO MULTITURN COILS IN 2D FINITE ELEMENT ANALYSIS

MSC/EMAS models can contain elements that represent each turn of wire, as has been demonstrated for one−turn primary and secondary windings (coils) on transformers attached to linear and nonlinear electronic circuits [6]. In common cases of many turns on each coil, one modeling technique is to represent each individual turn with individual conducting 1D LINE finite elements. The 0D circuit elements (RES, IND, and CAP) may then be attached to these line finite elements. However, such a model is impractical for coils with hundreds or thousands of turns. Moreover, many hundreds or thousands of nodes would be added to the finite element models, making them inefficient to solve.

A 2D multiturn coil technique proposed recently [4] is based upon the integral form of Faraday's Law:

$$V = -\frac{\partial}{\partial t}\int \vec{B} \cdot d\vec{s} \tag{1}$$

where the integrand is the flux linked by a coil in which the voltage V is induced. Using the definition of magnetic vector potential $\vec{A}$, we obtain:

$$V = -\frac{\partial}{\partial t}\int \nabla \times \vec{A} \cdot d\vec{s} \tag{2}$$

If $\vec{A}$ is continuous, then Stokes' theorem gives:

$$V = -\frac{\partial}{\partial t}\int \vec{A} \cdot d\vec{l} \tag{3}$$

where $d\vec{l}$ is the differential vector length of the coil, which for an N turn winding is N times that of a single−turn winding.

The technique based on (3) is to model multiple turns of a coil with conducting 1D line finite elements whose nodes are constrained to the same $\vec{A}$ as the nodes of the 2D finite ele-

ments, and whose lengths are proportional to the total number of turns modeled. The 0D circuit elements are then attached directly to the elongated 1D LINE elements.

NONLINEAR RLC CIRCUIT

Figure 1 shows an RLC circuit with a nonlinear L that has been analyzed previously by circuit techniques [7]. Figure 2 shows the applied voltage waveform [7], which is a square wave of period 50 microseconds. In this paper the circuit is analyzed by the finite element technique described above, employing 0D, 1D, and 2D finite elements in Solution 305.

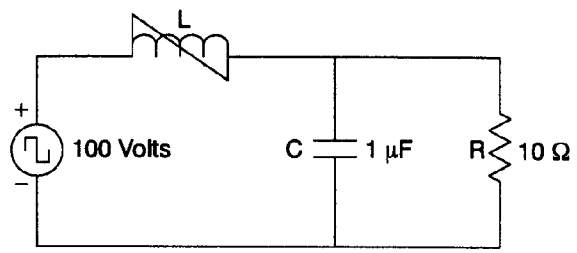

Figure 1: RLC circuit, where L is nonlinear.

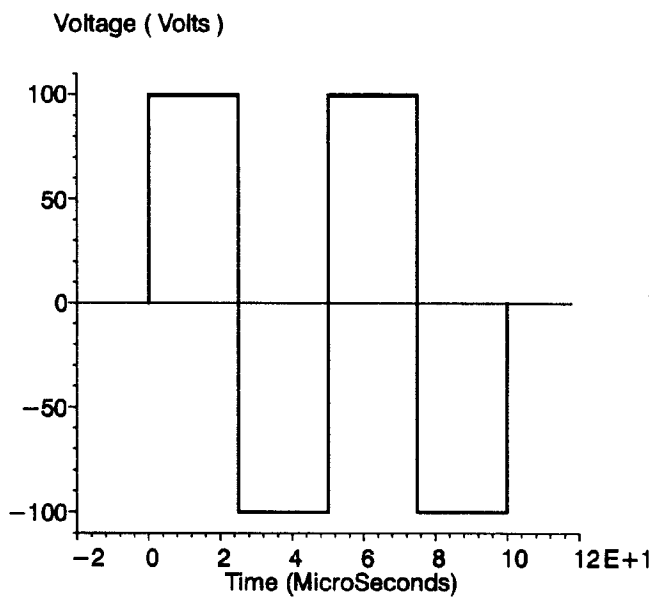

Figure 2: Input voltage waveform of Figure 1.

Figure 3 shows one example of inductor geometry [2] that can obtain the curve of flux linkage (λ) versus current (I) curve that is given in the previous work [7]. Note that no air gaps are present in this particular design of the magnetic core. The B−H curve of the magnetic material is proportional to the previously specified piecewise linear λ−I curve [7], and is shown in Figure 4.

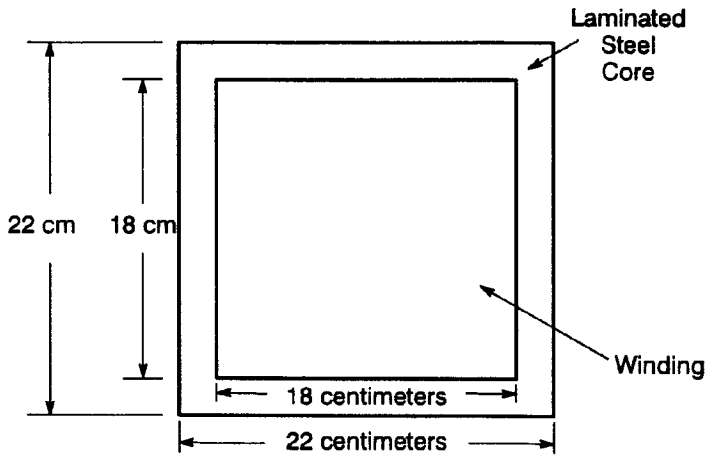

Figure 3: Geometry of inductor for Figure 1.

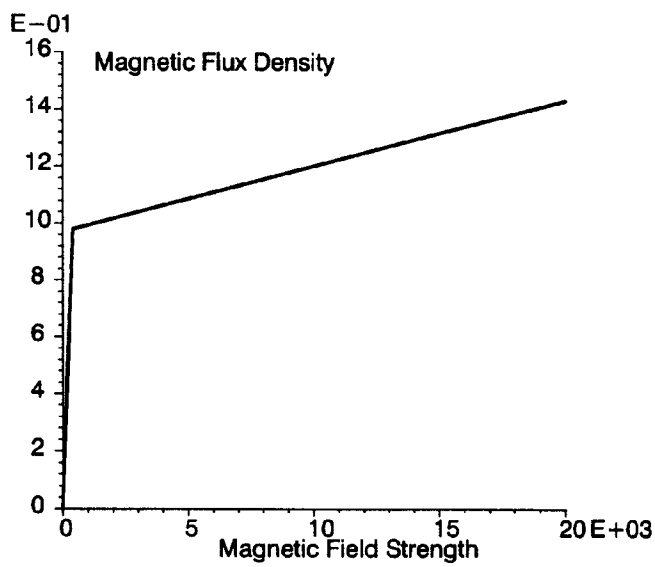

Figure 4: B−H curve assumed for core of Figure 3.

Figure 5 shows the MSC/EMAS model of Figure 2. The core is modeled with 2D finite elements, to which are attached 1D LINE elements to represent the multiturn coil and 0D finite elements that represent the R and C circuit elements. The square wave voltage excitation is transformed via Norton's theorem to a current source PCUR4 excitation in parallel with a RES element.

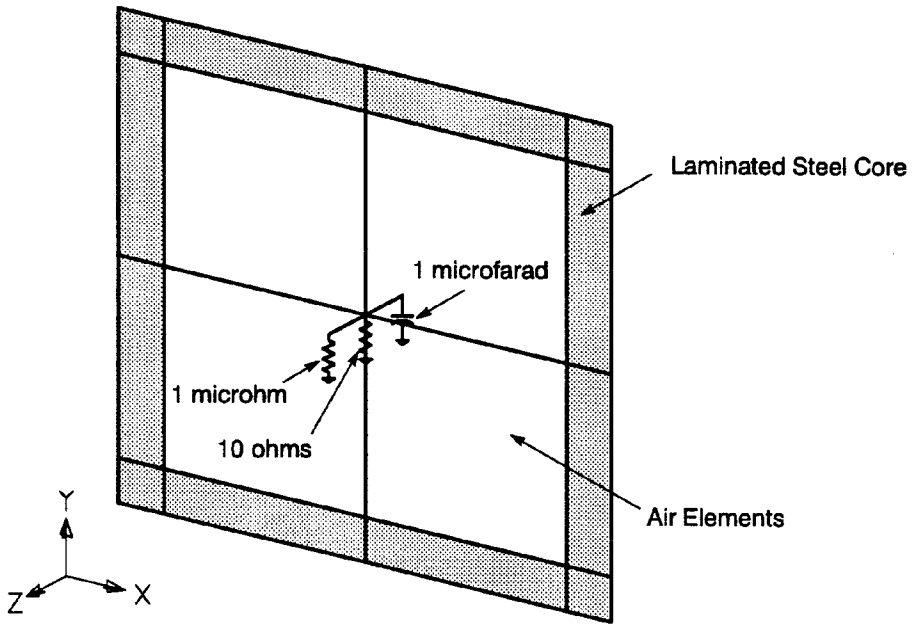

Figure 5: MSC/EMAS model of Figure 3.

Figure 6 shows the output voltage waveform (across the capacitor) computed by MSC/EMAS. The waveform appears to be identical to the waveform obtained by circuit analysis [7], thereby demonstrating the accuracy of MSC/EMAS.

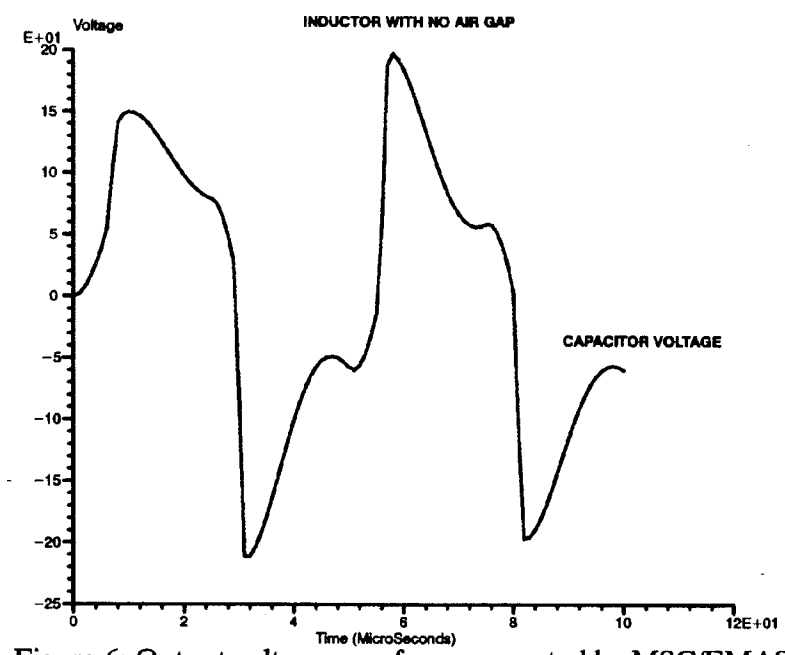

Figure 6: Output voltage waveform computed by MSC/EMAS.

The advantage of MSC/EMAS over circuit techniques is that the designer can easily investigate the effects of changes in geometry and materials. Figure 7 shows a new design of the inductor core. Note that for greater ease of assembly during manufacture, the new design

has two 1 mm air gaps which enable a bobbin–wound coil to be inserted in the inductor window. To attempt to account for the greater reluctance of the added air gaps, the core now has its legs thickened to twice their thickness of Figure 3. Another change in the design is that the core material has a finite conductivity of 1 S/m, which is typical of soft ferrites.

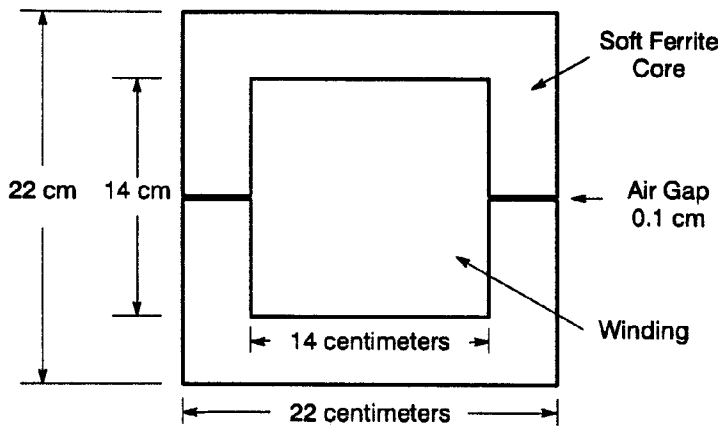

Figure 7: Geometry of new design of inductor.

Sol 305 results of MSC/EMAS for the new inductor design include average eddy current loss of approximately 100 watts. Figure 8 shows the computed capacitor voltage waveform. Note that the new waveform is considerably different from that of Figure 6. The engineer may therefore want to try other geometries and materials in subsequent finite element analyses to attempt to achieve the desired waveforms of voltage and current.

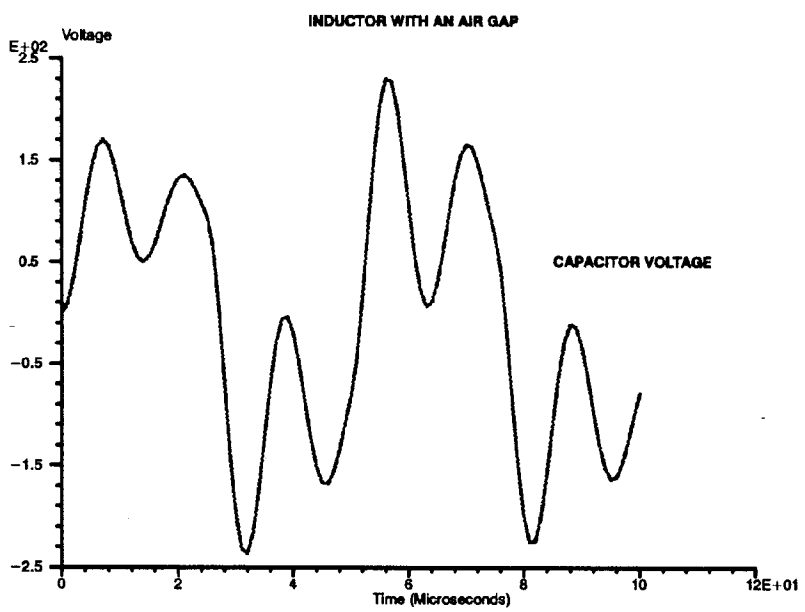

Figure 8: Output voltage waveform computed for inductor of Figure 7.

PROPOSED TECHNIQUE FOR 3D MULTITURN COILS

A 3D multiturn coil modeling technique proposed recently [5] is based upon the need to obtain the proper line integral of electric field $\vec{E}$ along the multiturn coil. In 3D problems $\vec{E}$ is a function of both the magnetic vector potential $\vec{A}$ and the time−integrated electric scalar potential ψ. The voltage induced in a coil is given by:

$$V = -\frac{\partial}{\partial t}\int(\vec{A} + \nabla\psi)\cdot d\vec{l} \tag{4}$$

where $\vec{l}$ is the vector length of the coil, which for an N turn coil is N times that of a single−turn coil. Here we **maintain the geometric shape and size** of the multiturn coil, but attach the 0D circuit to winding degrees of freedom that are constrained such that:

$$U_{i_{(winding)}} = N\, U_{i_{(3DModel)}} \tag{5}$$

where U_i is any component of $\vec{A}$ or ψ. This is a multipoint constraint (MPC) technique somewhat similar to the MPCs widely used for modeling periodic boundary conditions in electric machines [1]. However, periodic MPCs have a coefficient of +1 or −1, while the coefficient N of (5) is any real number. The MPC record in MSC/EMAS allows the users to enter a coefficient N that is an integer or non−integer number of turns.

DESCRIPTION OF 3D MULTITURN TRANSFORMER

Figure 9 shows a simple transformer with a four−turn secondary coil winding [4],[5]. The highly permeable core material forms a square path for the magnetic flux. To make this transformer approach an "ideal" transformer, the core material is assumed to have a permeability of 1×10^5 times that of air and a conductivity of zero. In this particular case, the primary coil has one turn and is energized with 120 volts at 60 Hz through a series resistor of 0.1 ohm. The secondary coil winding has a 2 ohm resistor across it.

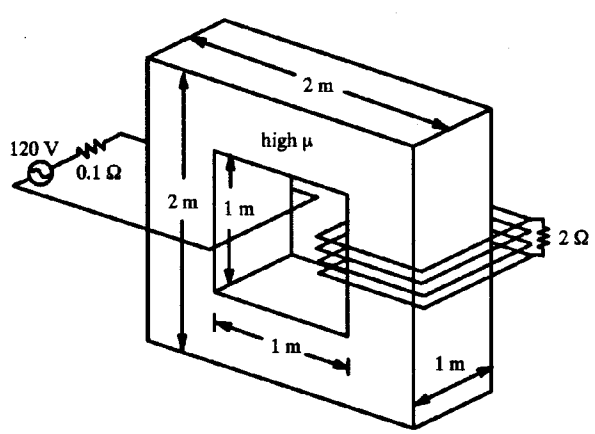

Figure 9: Geometry of 3D transformer with attached circuits.

The transformer of Figure 9 is first analyzed using ideal transformer theory. Since the turns ratio is 4, the impedance of the secondary is divided by $4^2 = 16$ when it is "referred"

to the primary. Thus the source sees a total resistance of 0.10 ohm plus (2/16) ohm, for a total input resistance of 0.225 ohm. The ideal primary current I_1 is thus:

$$120./(.225) = 533.333 \text{ amps} \angle\ 0°,$$

and the ideal secondary current I_2 is 1/4th the primary current, as listed in Table 1.

Table 1: Calculated Transformer Currents (in amps and degrees)

Model Core	μ_r	Seconday Winding	Winding Currents	
			I_1	I_2
IDEAL	infinity	ideal	$533.333 \angle 0°$	$133.333 \angle 0°$
A	1×10^5	rectangular	$533.5 \angle -1.121°$	$133.310 \angle 0.4568°$
B	500.	rectangular	$1128.08 \angle -12.17°$	$50.312 \angle 67.34°$
C	500.	non−rectangular	$1127.97 \angle -12.17°$	$50.372 \angle 67.35°$

3D LINEAR TRANSFORMER ANALYSES USING THE NEW MULTITURN TECHNIQUE

Figure 10 shows an MSC/EMAS model of Figure 9 that uses the constraint technique of (5). The model is made up of 3D HEXAs, 1D LINEs, and 0D RESs. The "halos" in Figure 10 contain the winding LINEs to which the 0D circuit elements are attached; the halos can be placed anywhere because the MPCs of (5) connect them to the rest of the finite element model. Table 1 model A lists the computed currents; they agree very well with ideal transformer theory. Figure 10 shows the computed leakage flux lines (at the instant the applied voltage is peaking).

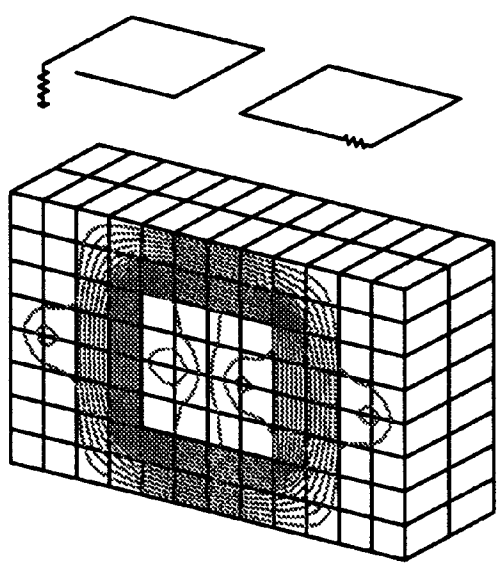

Figure 10: Model A of transformer and its flux lines.

Table 1 also lists a model B that is identical to that of Figure 10 except that the core material has been lowered to a relative permeability of 500. The currents are considerably changed due to the lower magnetizing inductance.

Figure 11 shows a finite element model C that is identical to that of model B in Figure 10 except that the secondary coil winding shape is now non–rectangular. Table 1 shows that the computed I_2 is now 0.12 % higher because of the smaller leakage flux of the enlarged non–rectangular secondary coil.

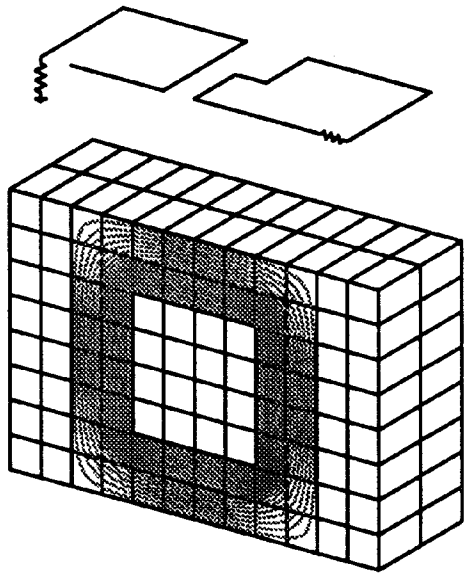

Figure 11: Model C and its flux lines.

3D NONLINEAR TRANSFORMER ANALYSES USING THE NEW MULTITURN TECHNIQUE

The transformer input voltage is now changed to the sawtooth waveform shown in Figure 12 of period 16 milliseconds (1/62.5 Hz) with 1200 volts peak, which is sufficient to cause saturation in the core. Using the model of Figure 10 with a typical steel B–H curve [1], nonlinear transient finite element analysis is employed to solve for the time–varying nonlinear fields and currents. The conductivity of the core is changed from the previous value of 0 to 1 S/m, which produces eddy current loss in the core.

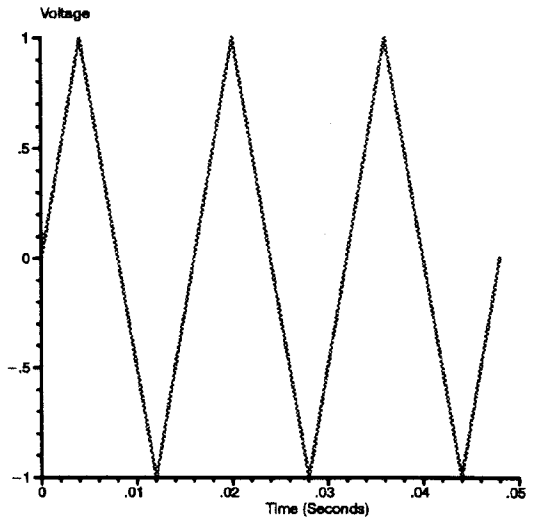

Figure 12: Applied voltage waveform for nonlinear transformer of Figure 9.

Figure 13 is a graph of the computed magnetic flux density waveform, which is seen to be clipped near the 1.5 T saturation knee of the core material. Figure 14 is a graph of the computed secondary current waveform. Note that it is "peaked" due to saturation. Figure 15 is a graph of computed eddy current core loss versus time.

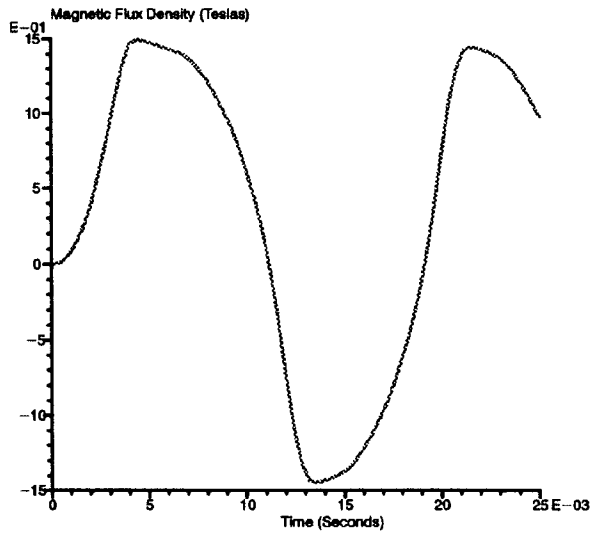

Figure 13: Computed waveforms for nonlinear transformer, B(t).

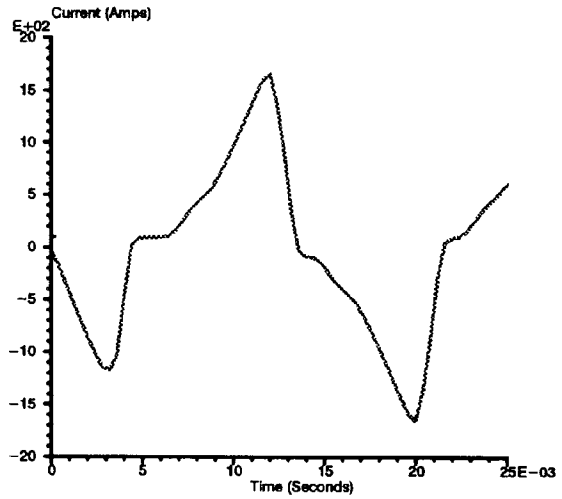

Figure 14: Computed waveforms for nonlinear transformer, $I_2(t)$.

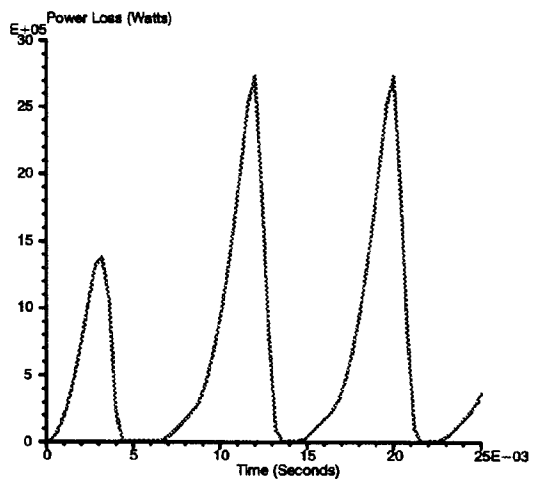

Figure 15: Eddy current loss vs time for nonlinear transformer.

INDUCTION MOTOR ANALYSIS WITH VOLTAGE EXCITATION

Induction motor currents at locked rotor (starting) can be very high. A known voltage, such as 230 V 60 Hz, is applied to the multiturn coils. The electrical engineer needs to compute the currents, which often must not exceed a specified maximum amperage.

Figure 16 shows an MSC/EMAS induction motor model. The stator windings are excited with a voltage source (Norton Equivalent). In this model the "halos" are 1−D line elements above the model. The voltage is applied to one end of the 1−D line element while the other end of the line is grounded. Each of these line elements is connected to the stator slots with MPCs. As with the transformer models, the coefficients of (5) on the MPCs account for multi−turn coils that are in the stator slots.

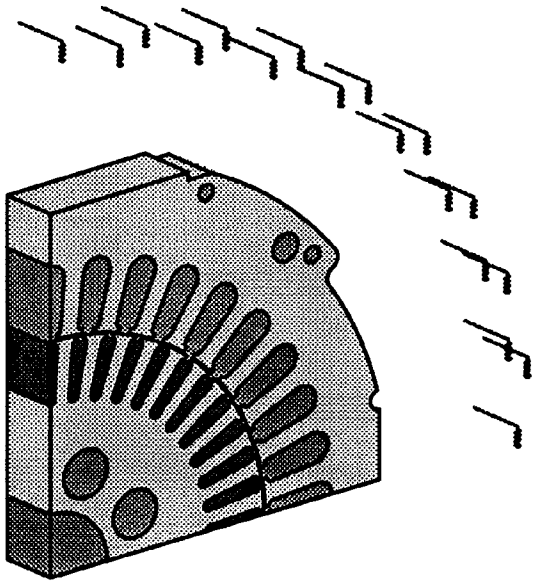

Figure 16: Induction motor.

Figure 17, shows the current for the stator windings. The currents shown are sinusoidal as expected [3] even with the high saturation in the rotor teeth. A flux plot for one time instant can be seen in figure 18.

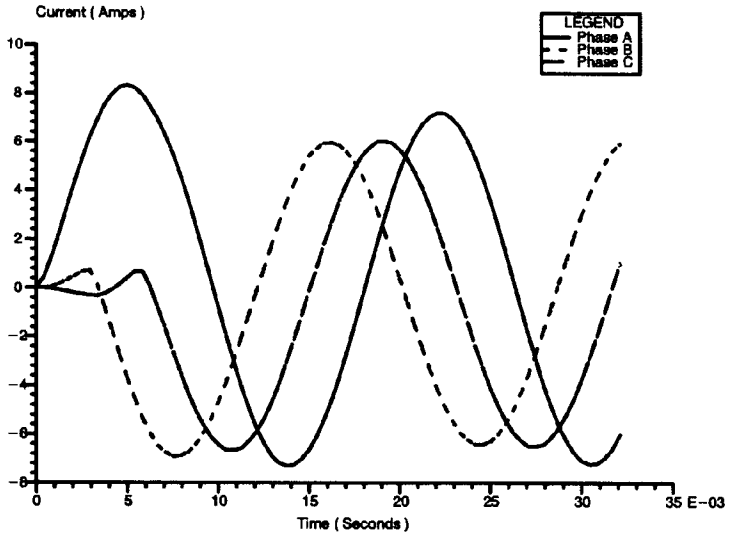

Figure 17: Locked Rotor Current for Induction Motor.

The rotor teeth can be highly saturated due to the high input currents and the induced currents in the rotor bars. The analysis, therefore, must be performed as nonlinear transient (Sol 305). These analyses have been difficult to run in the past due to problems with the smoothness of the B−H table, currents rising or falling too quickly, time steps being too large, etc. With Version 2.5 of MSC/EMAS, an alternative method for nonlinear transient solutions is available. This method, ADAPT, uses adaptive time stepping which will automatically

change the time step through bisections in order to achieve convergence. This becomes very useful in problems where the current changes very quickly. This new method eliminates the need to have thousands of time steps or multiple subcases because only one area of the excitation requires a small time step. The user can select a time step small enough to accommodate the majority of the excitation and let the nonlinear transient solver decrease the time step, if necessary, to achieve convergence in areas where a smaller time step is required.

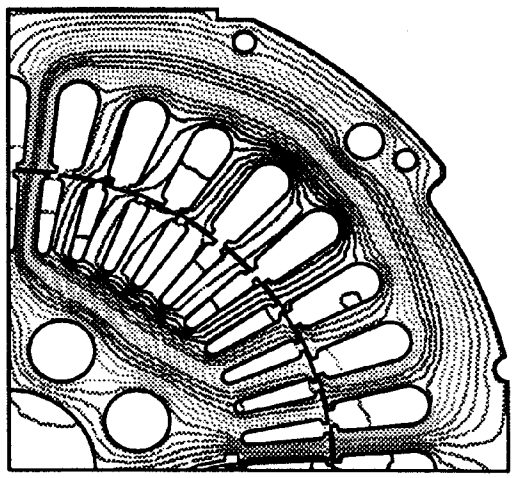

Figure 18: Induction Motor and its flux lines.

CONCLUSION

MSC/EMAS models have been presented that represent multiturned coils in 2D and 3D finite element models with attached electric circuits. The voltage and current wave forms computed by MSC/EMAS in a nonlinear RLC circuit agree with those computed elsewhere. Analysis of an ideal transformer obtains primary and secondary currents that agree very closely with those of ideal transformer theory. Analyzing a nonlinear transformer with Sol 305 gives results that appear reasonable. Sol 305 analysis of an induction motor gives good results for the stator winding currents and shows the advantage of the new adaptive time stepping approach available in MSC/EMAS Version 2.5.

REFERENCES

[1] Brauer, John R. (ed.), What Every Engineer Should Know About Finite Element Analysis, 2nd edition, Marcel Dekker, Inc., New York, 1993.

[2] Brauer, John R., "Finite Element Analysis of Power Electronic Circuits Containing Nonlinear Magnetic Components," *Digest of IEEE Applied Power Electronics Conference*, March 7–11, 1993.

[3] Brauer, John R., "Saturation Harmonics and Current Waveforms of Single–Phase Induction Motors," *IEEE Trans. on Power Apparatus & Systems.*, January 1975.

[4] Brauer, John R. and MacNeal, Bruce E., "Finite element modeling of multiturn windings with attached electric circuits," *IEEE Trans. on Magnetics*, v. 29, March 1993, in press.

[5] Brauer, John R., MacNeal, Bruce E. and Hirtenfelder, Franz, "New Constraint Technique for 3D Finite Element Analysis of Multiturn Windings with Attached Circuits," *Digest of IEEE INTERMAG Conference*, Stockholm, Sweden, April 13–16, 1993.

[6] "MSC/EMAS Application Manual, Version 2, Sections 2.1.3 and 5.1.2, The MacNeal–Schwendler Corporation, Los Angeles, CA, 1993."

[7] Nelms, R. M. and Grigsby, L. L., "Simulation of power electronic circuits containing nonlinear inductances," *IEEE Trans. Aerospace & Electronic Systems*, pp. 924–931, Nov. 1991.